Journal of Microscopy, Vol. 210, Pt 3 June 2003, pp. 247–251
Received 10 August 2002; accepted 25 October 2002

Excitation dynamics in a three-quantum dot system driven by optical near-field interaction: towards a nanometric photonic device

K. KOBAYASHI*, S. SANGU*, A. SHOJIGUCHI*,
T. KAWAZOE*, K. KITAHARA† & M. OHTSU*,‡
**ERATO Localized Photon Project, Japan Science and Technology, 687-1 Tsuruma, Machida-shi, Tokyo 194-0004, Japan*
†Division of Natural Sciences, International Christian University, Tokyo, Japan
‡Interdisciplinary Graduate School of Science and Engineering, Tokyo Institute of Technology, Kanagawa, Japan

Key words. Coherent dynamics, nanometric photonic device, optical near-field interaction, phonon relaxation, Yukawa function, effective finite-range interaction.

Summary

Using density operator formalism, we discuss interdot excitation energy transfer dynamics driven by the optical near-field and phonon bath reservoir, as well as coherent excitation dynamics of a quantum dot system. As an effective interaction between quantum dots induced by the optical near-field, the projection operator method gives a renormalized dipole interaction, which is expressed as a sum of the Yukawa functions and is used as the optical near-field coupling of quantum dots. We examine one- and two-exciton dynamics of a three-quantum dot system suggesting a nanometric photonic switch, and numerically obtain a transfer time comparable with the recent experimental results for CuCl quantum dots.

1. Introduction

In near-field optical microscopy and spectroscopy, localization and tunneling of photons have played essential roles in spatial resolution beyond the diffraction limit. They are now recognized as key issues for nano and atom photonics (Ohtsu *et al.*, 2002), and it is very important to experimentally achieve local manipulation and control of the quantum states of an atom, molecule or quantum dot (QD) (Shojiguchi *et al.*, 2003). In this respect, coherent dynamics with dephasing of such a system driven by the optical near-field should be thoroughly investigated from the theoretical viewpoint. At the same time, we need to explore an intuitive understanding of the coherent excitation dynamics of QD systems and of their clear differences driven by either the far- or near-field.

Correspondence: K. Kobayashi. Tel.: +81 42 788 6036; fax: +81 42 788 6031; e-mail: kkoba@ohtsu.jst.go.jp

The purpose of this study is to theoretically address the above issues, in particular, the interdot excitation energy transfer via the optical near-field and the coherent excitation dynamics of a QD system. We follow an effective interaction picture to provide a systematic, consistent and quantitative method. Using an example of a three-QD system, we examine the one- and two-exciton dynamics driven by the optical near-field that competes with the exciton–phonon interaction, and compare the time scale required for the transfer with recent experimental work (Kawazoe *et al.*, 2002, 2003). On the basis of this analysis, an optical near-field nano-switch is proposed as a fundamental building block of nano photonics.

The paper is organized as follows. Section 2 discusses the optical near-field interaction between QDs, which is responsible for the interdot excitation energy transfer, from an effective interaction viewpoint. We then examine the excitation dynamics of a three-QD-system driven by the optical near-field interaction as well as the phonon interaction in Section 3. Section 4 gives some numerical results obtained from the equation of motion, followed by a proposal of a nano-switch based on the interdot excitation energy transfer in Section 5. Finally, concluding remarks are presented in Section 6.

2. Optical near-field interaction between quantum dots as an effective interaction and the interdot excitation energy transfer

According to the theoretical framework developed in our previous studies (Kobayashi & Ohtsu, 1999; Kobayashi *et al.*, 2001; Sangu *et al.*, 2001; Ohtsu *et al.*, 2002), let us consider an interdot interaction due to the optical near-field. The total Hamiltonian $\hat{H}$ for the system consists of $\hat{H}_{\text{photon}}$ for incident photons, $\hat{H}_{\text{matter}}$ for a surrounding macroscopic matter system,

$\hat{H}_{\rm QD}$ for a nanometric QD system, and their interactions $\hat{V}$ as given by the multipolar QED Hamiltonian (Cohen-Tannoudji *et al.*, 1989; Craig & Thirunamachandran, 1998; Andrews & Demidov, 1999).

$$\hat{H} = \hat{H}_{\rm photon} + \hat{H}_{\rm matter} + \hat{H}_{\rm QD} + \hat{V},$$
$$\hat{V} = -\sum_i \hat{\vec{\mu}}_i \cdot \hat{\vec{D}}(\vec{r}_i), \tag{1}$$

where $\hat{\vec{\mu}}_i$ denotes the dipole operator of either constituents of the macroscopic matter system or each QD, and $\hat{\vec{D}}(\vec{r}_i)$ represents the electric displacement vector at position $\vec{r}_i$. It is convenient to treat this kind of problem in two stages. First, the photons and macroscopic matter system are described on an equal basis in terms of a so-called polariton basis. The interaction between the QD system and the macroscopic system is then expressed using the polariton basis as

$$\hat{H} = \hat{H}_0 + \hat{V}' = \sum_{\vec{k}} E(k)\hat{\xi}^\dagger_{\vec{k}}\hat{\xi}_{\vec{k}} + \sum_\alpha E_\alpha \hat{B}^\dagger_\alpha \hat{B}_\alpha - \sum_\alpha \hat{\vec{\mu}}_\alpha \cdot \hat{\vec{D}}(\vec{r}_\alpha),$$
$$\hat{\vec{D}}(\vec{r}_\alpha) = i\sqrt{\frac{2\pi\hbar}{V}}\sum_{\vec{k}\lambda}\vec{e}_{\vec{k}\lambda} f(k)[\hat{\xi}_{\vec{k}}\, e^{i\vec{k}\cdot\vec{r}_\alpha} - \hat{\xi}^\dagger_{\vec{k}}\, e^{-i\vec{k}\cdot\vec{r}_\alpha}]. \tag{2}$$

Here the creation and annihilation operators of the polariton with wave vector $\vec{k}$ and eigenenergy $E(k)$ are denoted as $\hat{\xi}^\dagger_{\vec{k}}$ and $\hat{\xi}_{\vec{k}}$, whereas those of excitons in QD α are designated as $\hat{B}^\dagger_\alpha$ and $\hat{B}_\alpha$, with E_α being the exciton energy. The electric displacement vector is expanded in terms of the polariton basis and the coupling coefficient $f(k)$ between the macroscopic matter system and photons with polarization vector $\vec{e}_{\vec{k}\lambda}$. The Planck constant divided by 2π and the normalization volume are $\hbar$ and V, respectively. The coupling coefficient $f(k)$ can be written as

$$f(k) = \frac{\hbar c k}{\sqrt{\hbar E(k)}}\sqrt{\frac{E(k)^2 - E_m^2}{2E(k)^2 - E_m^2 - (\hbar c k)^2}}, \tag{3}$$

where c and E_m are the velocity of light in a vacuum and the excitation energy of the macroscopic matter system, respectively.

Although the Hamiltonian of Eq. (2) provides a variety of information about both static and dynamic properties of the system, here we restrict ourselves to exploring the interaction between QDs. Then it is more practical to use some of eigenstates $\left|\Psi^P_\lambda\right\rangle$ of $\hat{H}_0$, instead of exact eigenstates $\left|\Psi_\lambda\right\rangle$ of $\hat{H}$, and an effective interaction operator $\hat{V}_{\rm eff}$ that satisfies the following relation

$$\left\langle \Psi^P_f \middle| \hat{V}_{\rm eff} \middle| \Psi^P_i \right\rangle = \left\langle \Psi_f \middle| \hat{V} \middle| \Psi_i \right\rangle. \tag{4}$$

These procedures are carried out on the basis of the projection operator method, as discussed previously in detail. When we set the relevant initial and final states in P-space to $\left|\Psi^P_i\right\rangle = \left|A^*\right\rangle\left|B\right\rangle\left|0\right\rangle$ and $\left|\Psi^P_f\right\rangle = \left|A\right\rangle\left|B^*\right\rangle\left|0\right\rangle$, with $\left|\alpha\right\rangle$, $\left|\alpha^*\right\rangle$ ($\alpha = A,B$) and $\left|0\right\rangle$ being the ground, excited states of QDs and the vacuum state of the polaritons, the effects of both the photons and the macroscopic matter system, i.e. the polaritons, are renormalized into an effective two-body interaction between QDs. We call this effective interaction the optical near-field interaction or coupling which is explicitly given as

$$\begin{aligned}\hbar U(r) &\equiv \left\langle \Psi^P_f \middle| \hat{V}_{\rm eff} \middle| \Psi^P_i \right\rangle \\ &= -\frac{\mu_A\mu_B}{6\pi^2}\int d^3k\, f^2(k)\left\{\left[\frac{1}{E(k)+E_A} + \frac{1}{E(k)+E_B}\right]e^{i\vec{k}\cdot\vec{r}}\right. \\ &\quad \left. + \left[\frac{1}{E(k)-E_A} + \frac{1}{E(k)-E_B}\right]e^{-i\vec{k}\cdot\vec{r}}\right\} \\ &= \frac{\mu_A\mu_B}{3(\hbar c)^2}\sum_{\alpha=A}^{B}\left[W_{\alpha+}Y(\Delta_{\alpha+}r) + W_{\alpha-}Y(\Delta_{\alpha-}r)\right],\end{aligned} \tag{5}$$

where the transition dipole moments of the relevant QDs A and B are denoted as μ_A and μ_B, respectively. In addition, $W_{\alpha\pm}$ denotes the weight factor of each Yukawa function defined as

$$Y(\Delta_{\alpha\pm}r) = \frac{\exp[-\Delta_{\alpha\pm}r]}{r},$$
$$\Delta_{\alpha\pm} = \frac{1}{\hbar c}\sqrt{2E_p(E_m \pm E_\alpha)}, \tag{6}$$

with the interdot distance $r = \left|\vec{r}_A - \vec{r}_B\right|$, the polariton effective mass rewritten as $E_p = m_p c^2$. The factor $\Delta_{\alpha-}$ becomes either real or pure imaginary depending on the magnitude of E_m and E_α, which means that this component behaves as either a localized or propagation mode. We are primarily interested in the localized mode, and also neglected two additional terms in Eq. (5) that are independent of the QD parameters as a far-field contribution. Here it should be noted that the optical near-field coupling $U(r)$ could induce the interdot energy transfer process when the neighbouring QDs have resonant levels, i.e. $E_A = E_B$.

3. Excitation dynamics driven by both optical near-field and phonon interactions

In the preceding section, we focused on the optical near-field interaction between QDs. However, phonon effects on the coherent excitation dynamics of a QD system cannot be excluded. Using an example of a three-QD system shown schematically in Fig. 1, we discuss how the interdot excitation energy and quantum coherence are transferred under the optical near-field and the phonon interactions with the QDs. The model Hamiltonian of such a system can be written as

$$\hat{H} = \hat{H}_0 + \hat{V}_{\rm NF} + \hat{V}_{\rm vib},\ \hat{H}_0 = \hat{H}_{\rm QD} + \hat{H}_{\rm ph},$$
$$\hat{H}_{\rm QD} = E_2\hat{D}^\dagger\hat{D} + E_1\hat{A}^\dagger_1\hat{A}_1 + (E_2 - E_1)\hat{C}^\dagger\hat{C} + E_1\hat{A}^\dagger_2\hat{A}_2,$$
$$\hat{H}_{\rm ph} = \sum_n \varepsilon_n \hat{b}^\dagger_n \hat{b}_n,$$
$$\hat{V}_{\rm NF} = \hbar U(r_{12})(\hat{D}^\dagger\hat{A}_1\hat{C} + \hat{D}\hat{C}^\dagger\hat{A}^\dagger_1) + \hbar U(r_{23})(\hat{A}^\dagger_1\hat{A}_2 + \hat{A}_1\hat{A}^\dagger_2)\hat{C}\hat{C}^\dagger,$$
$$\hat{V}_{\rm vib} = \sum_n \hbar\,(g_n\hat{b}^\dagger_n\hat{C} + g^*_n\hat{b}_n\hat{C}^\dagger), \tag{7}$$

where $\hat{H}_{\rm QD}$, $\hat{H}_{\rm ph}$, $\hat{V}_{\rm NF}$, and $\hat{V}_{\rm vib}$ describe the isolated QD excitons, the phonon bath reservoir, optical near-field interaction and exciton–phonon interaction, respectively. The eigenenergies

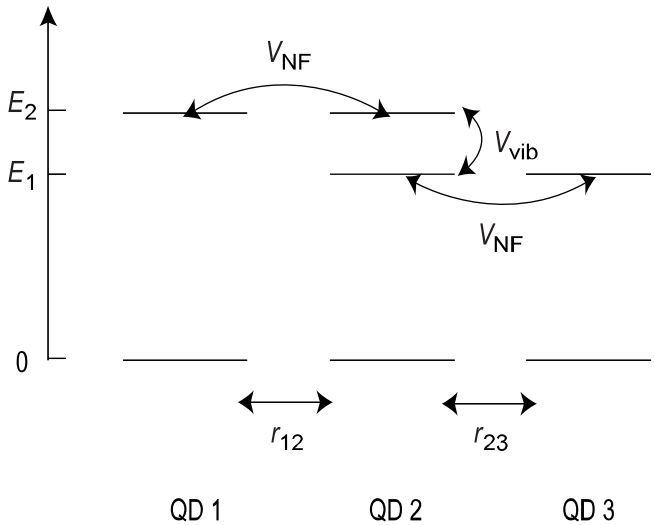

Fig. 1. Three-QD system coupled via optical near-field (V_{NF}) and phonon (V_{vib}) interactions. The horizontal lines represent energy levels of each QD, and the distance between two neighbouring QDs is denoted as $r_{12}(r_{23})$.

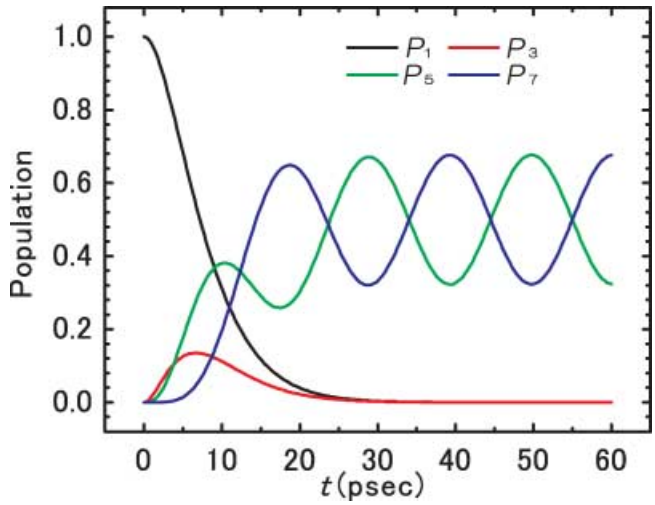

Fig. 2. One-exciton dynamics. The population probabilities of P_1, P_3, P_5, and P_7, corresponding to the operators $\hat{O}(1), \hat{O}(3), \hat{O}(5)$, and $\hat{O}(7)$ are plotted as a function of time. The operator $\hat{O}(1)$ represents a one-exciton state in QD 1, $\hat{O}(3)$ and $\hat{O}(5)$ describe one-exciton in the E_2 and E_1 level in QD 2, respectively, and $\hat{O}(7)$ describes one in QD 3.

of each QD and the phonon levels are denoted as E_1, E_2, and ε_n, whereas g_n denotes the QD–phonon bath coupling constant. The operators $(\hat{D}^\dagger, \hat{D})$, $(\hat{A}_2^\dagger, \hat{A}_2)$, and $(\hat{A}_1^\dagger, \hat{A}_1)$ are fermionic operators for the creation and annihilation of an exciton in QD 1, QD 3 and the lower energy level of QD 2, respectively, while the fermionic operators $(\hat{C}^\dagger, \hat{C})$ and the bosonic operators $(\hat{b}_n^\dagger, \hat{b}_n)$ are for the $(E_2 - E_1)$ level of QD 2 and for the phonon bath reservoir, respectively. The equation of motion describing the dynamics of the system can be obtained using Born–Markov approximation (Carmichael, 1999) as

$$\frac{\partial \hat{\rho}(t)}{\partial t} = \frac{1}{i\hbar}[\hat{V}_{NF}, \hat{\rho}(t)] - \frac{\gamma}{2}(\{\hat{C}^\dagger\hat{C}, \hat{\rho}(t)\} - 2\hat{C}\hat{\rho}(t)\hat{C}^\dagger), \qquad (8)$$

where we trace out the degrees of freedom of the phonon bath reservoir, and define the density operator of the QD system in the interaction representation as $\hat{\rho}(t)$, representing the relaxation constant as γ. In order to solve Eq. (8), we use the following expansion for the density operator, instead of the usual density matrix form:

$$\hat{\rho}(t) = \sum_\ell P_\ell(t)\hat{O}(\ell), \qquad (9)$$

where $P_\ell(t)$ refers to the occurrence probability of the state defined by the operator $\hat{O}(\ell)$. As shown in Table 1, the operator $\hat{O}(\ell)$ is related to either the number of excitons occupied in the system or the quantum coherence of the system, and it is suitable for examining one-exciton dynamics, two-exciton dynamics and so forth.

4. Numerical results

We show some numerical results obtained from Eqs (8) and (9) in order to discuss the exciton dynamics of the system illustrated in Fig. 1. In the following we assume cubic CuCl QDs embedded in NaCl matrix whose physical quantities are cited from the references (Hanamura, 1988; Kataoka *et al.*, 1993; Sakakura & Masumoto, 1997). Figure 2 presents an example of one-exciton dynamics that illustrates how fast an exciton located in QD 1 at time $t = 0$ is transferred to QD 3. It follows from the figure that it takes about 10–20 ps under the condition of $\hbar\gamma = 160\,\mu\text{eV}$, $\hbar U(r_{12}) = \hbar U(r_{23}) = 40\,\mu\text{eV}$. This condition was estimated from Eq. (5) for CuCl QDs with a size of 5 nm arranged equidistantly at 10 nm, and with transition

Table 1. Explicit expressions for the operator $\hat{O}(\ell)$.

One-exciton part	Two-exciton part	Quantum coherence part
$\hat{O}(1) = \hat{D}^\dagger\hat{D}\hat{A}_1\hat{C}\hat{A}_1^\dagger\hat{C}^\dagger\hat{A}_2\hat{A}_2^\dagger$,	$\hat{O}(2) = \hat{D}^\dagger\hat{D}\hat{A}_1\hat{C}\hat{A}_1^\dagger\hat{C}^\dagger\hat{A}_2^\dagger\hat{A}_2$	$\hat{O}(c1) = \frac{i}{\sqrt{2}}(\hat{D}^\dagger\hat{A}_1\hat{C} - \hat{D}\hat{A}_1^\dagger\hat{C}^\dagger)\hat{A}_2\hat{A}_2^\dagger$, $\hat{O}(c2) = \frac{i}{\sqrt{2}}(\hat{D}^\dagger\hat{A}_1\hat{C} - \hat{D}\hat{A}_1^\dagger\hat{C}^\dagger)\hat{A}_2^\dagger\hat{A}_2$
$\hat{O}(3) = \hat{D}\hat{D}^\dagger\hat{A}_1^\dagger\hat{C}^\dagger\hat{A}_1\hat{C}\hat{A}_2\hat{A}_2^\dagger$,	$\hat{O}(4) = \hat{D}\hat{D}^\dagger\hat{A}_1^\dagger\hat{C}^\dagger\hat{A}_1\hat{C}\hat{A}_2^\dagger\hat{A}_2$	$\hat{O}(c3) = \hat{D}^\dagger\hat{D}\frac{i(\hat{A}_1^\dagger\hat{A}_2 - \hat{A}_1\hat{A}_2^\dagger)}{\sqrt{2}}\hat{C}\hat{C}^\dagger$, $\hat{O}(c4) = \hat{D}\hat{D}^\dagger\frac{i(\hat{A}_1^\dagger\hat{A}_2 - \hat{A}_1\hat{A}_2^\dagger)}{\sqrt{2}}\hat{C}\hat{C}^\dagger$
$\hat{O}(5) = \hat{D}\hat{D}^\dagger\hat{A}_1^\dagger\hat{C}\hat{A}_1\hat{C}^\dagger\hat{A}_2\hat{A}_2^\dagger$,	$\hat{O}(6) = \hat{D}^\dagger\hat{D}\hat{A}_1^\dagger\hat{C}\hat{A}_1\hat{C}^\dagger\hat{A}_2\hat{A}_2^\dagger$	
$\hat{O}(7) = \hat{D}\hat{D}^\dagger\hat{A}_1\hat{C}\hat{A}_1^\dagger\hat{C}^\dagger\hat{A}_2^\dagger\hat{A}_2$,	$\hat{O}(8) = \hat{D}\hat{D}^\dagger\hat{A}_1^\dagger\hat{C}\hat{A}_1\hat{C}^\dagger\hat{A}_2^\dagger\hat{A}_2$	$\hat{O}(c5) = \frac{i}{\sqrt{2}}(\hat{D}^\dagger\hat{C}\hat{A}_2 + \hat{D}\hat{C}^\dagger\hat{A}_2^\dagger)\hat{A}_1^\dagger\hat{A}_1$
$\hat{O}(9) = \hat{D}\hat{D}^\dagger\hat{A}_1\hat{C}\hat{A}_1^\dagger\hat{C}^\dagger\hat{A}_2\hat{A}_2^\dagger$		

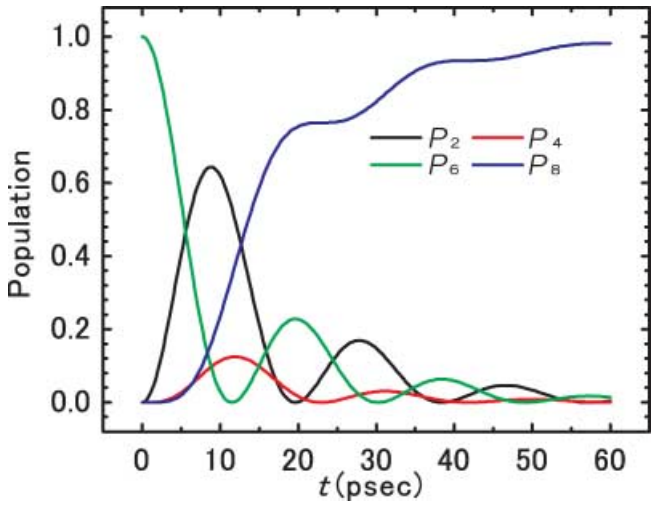

Fig. 3. Two-exciton dynamics. The time evolution of the population probabilities of P_2, P_4, P_6, and P_8 are plotted, similar to Fig. 2. Initially, one exciton exists in QD 1 and another in QD 2, denoted as $P_6(0) = 1$. The probability P_8 shows exciton transfer from QD 1 to QD 3 when an exciton exists in QD 2.

dipole moments of $\mu_A = \mu_B = 0.29\ (\mathrm{eV} \cdot \mathrm{nm}^3)^{1/2}$. The theoretically estimated time scale is found to be consistent with the recent experimental results (Kawazoe *et al.*, 2002a,b). Moreover, nutation can be seen in $P_5(t)$ and $P_7(t)$, owing to the quantum coherence between QDs 2 and 3.

Figure 3 depicts an example of two-exciton dynamics under the initial condition that one exciton exists in QD 1 and another in QD 2 at time $t = 0$, i.e. $P_6(0) = 1$. The other conditions are the same as used in Fig. 2. The probability $P_8(t)$ in Fig. 3 shows that exciton transfer from QD 1 to QD 3 takes place in less than 60 ps when an exciton exists in QD 2. The exciton, or excitation energy, is transferred via the quantum coherences $\hat{O}(c3)$, $\hat{O}(c7)$, and $\hat{O}(c2)$ driven by the optical near-field interaction. This coincides with the oscillations with a period of about 20 ps in $P_2(t)$, $P_4(t)$, and $P_8(t)$, as well as $P_6(t)$, although they are damped due to the phonon relaxation. It should be noted that the first peak shift between $P_2(t)$ and $P_4(t)$ originated from the fermionic nature of the exciton in QD 2. In addition, the decay rate of the quantum coherence of the three-QD system is half that of the two-QD system, and this fact suggests a possibility of controlling the relaxation time and the excitation transfer time via quantum coherence.

5. Three-QD system as a building block of a nanometric photonic switch based on interdot excitation energy transfer

Applying the above considerations to a nanometric photonic device, one may have a building block for a photonic switch as illustrated in Fig. 4. It consists of three QDs (QD-I, QD-O, QD-C), and each of the two neighbouring QD pairs has a resonant energy level coupled by the optical near-field. The signal transmission relies on the excitation energy transfer from QD-I to

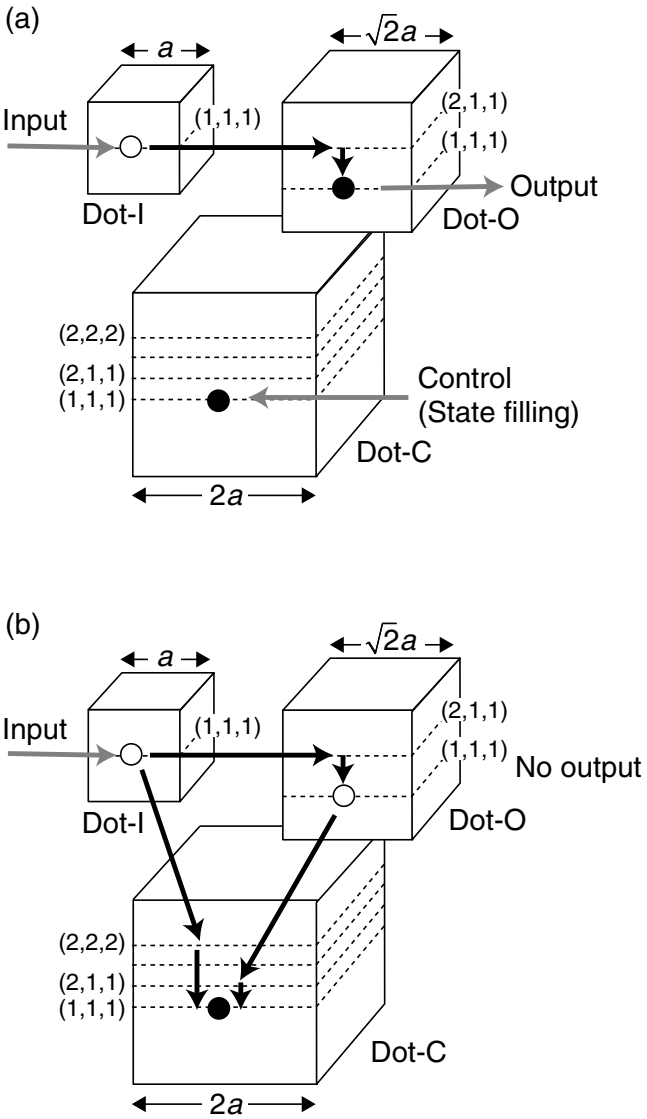

Fig. 4. Building block composed of three QDs for a photonic switch showing (a) ON, (b) OFF states. As indicated by arrows, input population in QD-I is transferred to QD-O, whose signal is detected either by near-field coupling to the detector or by far-field light.

QD-O via the optical near-field interaction. The control field applied to QD-C governs the optical near-field interaction between QD-I and QD-C, as well as QD-O and QD-C, and provides the switching mechanism. In the ON state of the switch (Fig. 4a), the signal transmission to QD-C is blocked by the state filling effect of (1,1,1) level in QD-C, and the input energy from QD-I is directed to QD-O resulting in the output signal that can be detected either by near-field coupling to the detector or by far-field light emitted with electron-hole recombination. By contrast, the input signal in the OFF state is collected at QD-C as a result of the optical near-field and exciton–phonon coupling, which leads to no output signal in QD-O. The switching speed of the device is estimated as a few to a

hundred picoseconds similar to the time scale obtained in Fig. 3, although it depends on the material, size, and spacing of the QDs.

6. Concluding remarks

Towards the realization of nanometric photonic devices, we investigated the dynamics of a nanometric QD system under the competition of the optical near-field and phonon interactions, from the effective interaction picture to provide a systematic and consistent method of analysing the optical near-field interaction quantitatively. Using the example of a three-QD system, we examined one- and two-exciton dynamics, both of which show that excitation energy transfer from QD 1 to QD 3 occurs in a few tens of picoseconds. This time scale is consistent with the experimental results obtained with CuCl QDs. By utilizing the theoretical results obtained, a photonic switch as a new scheme of nano-photonic device based on interdot excitation energy transfer via optical near-fields has been suggested. Owing to the page limit, a detail analysis on the device will be published elsewhere (see, for example, Sangu *et al.*, 2003).

References

Andrews, D.L. & Demidov, A.A. (1999) *Resonance Energy Transfer*. Wiley, Chichester.

Carmichael, H.J. (1999) *Statistical Methods in Quantum Optics 1*. Springer, Berlin.

Cohen-Tannoudji, C., Dupont-Roc, J. & Grynberg, G. (1989) *Photons and Atoms*. Wiley, New York.

Craig, D.P. & Thirunamachandran, T. (1998) *Molecular Quantum Electrodynamics*. Dover Publications, New York.

Hanamura, E. (1988) Very large optical nonlinearity of semiconductor micro-crystallites. *Phys. Rev. B*, **37**, 1273–1279.

Kataoka, T., Tokizaki, T. & Nakamura, A. (1993) Mesoscopic enhancement of optical nonlinearity in CuCl quantum dots: giant-oscillation strength effect on confined excitons. *Phys. Rev. B*, **48**, 2815–2818.

Kawazoe, T., Kobayashi, K., Lim, J., Narita, Y. & Ohtsu, M. (2002) Direct observation of optically forbidden energy transfer between CuCl quantum cubes via near-field optical spectroscopy. *Phys. Rev. Lett.* **88**, 067404–067401-4.

Kawazoe, T., Kobayashi, K., Sangu, S. & Ohtsu, M. (2003) Demonstrating nanophotonic switching operation by near-field pump-probe photoluminescence spectroscopy of CuCl quantum cubes. *J. Microsc.*

Kobayashi, K. & Ohtsu, M. (1999) Quantum theoretical approach to a near-field optical system. *J. Microsc.* **194**, 249–254, and references therein.

Kobayashi, K., Sangu, S., Ito, H. & Ohtsu, M. (2001) Near-field optical potential for a neutral atom. *Phys. Rev. A*, **63**, 013806–1–9.

Ohtsu, M., Kobayashi, K., Kawazoe, T., Sangu, S. & Yatsui, T. (2002) Nanophotonics: design, fabrication, and operation of nanometric devices using optical near fields. *IEEE J. Selected Topics Quantum Electron.* **8**, 839–862.

Sakakura, N. & Masumoto, Y. (1997) Persistent spectral-hole-burning spectroscopy of CuCl quantum cubes. *Phys. Rev. B*, **56**, 4051–4055.

Sangu, S., Kobayashi, K. & Ohtsu, M. (2001) Optical near fields as photon-matter interacting systems. *J. Microsc.* **202**, 279–285.

Sangu, S., Kobayashi, K., Shojiguchi, A., Kawazoe, T. & Ohtsu, M. (2003) Excitation energy transfer and population dynamics in a quantum dot system induced by optical near-field interaction. *J. Appl. Phys.* **93**, 2937–2945.

Shojiguchi, A., Kobayashi, K., Sangu, S., Kitahara, K. & Ohtsu, M. (2003) Coherent dipole oscillation induced by localized photons. *Nonlinear Optics*, and references therein.